

Solving Kepler's equation CORDIC-like

M. Zechmeister¹

Institut für Astrophysik, Georg-August-Universität, Friedrich-Hund-Platz 1, 37077 Göttingen, Germany
e-mail: zechmeister@astro.physik.uni-goettingen.de

Received / Accepted

ABSTRACT

Context. Many algorithms to solve Kepler's equations require the evaluation of trigonometric or root functions.

Aims. We present an algorithm to compute the eccentric anomaly and even its cosine and sine terms without usage of other transcendental functions at run-time. With slight modifications it is applicable for the hyperbolic case, too.

Methods. Based on the idea of CORDIC, it requires only additions and multiplications and a short table. The table is independent of eccentricity and can be hardcoded. Its length depends on the desired precision.

Results. The code is short. The convergence is linear for all mean anomalies and eccentricities e (including $e = 1$). As a stand-alone algorithm, single and double precision is obtained with 29 and 55 iterations, respectively. One half or two third of the iterations can be saved in combination with Newton's or Halley's method at the cost of one division.

Key words. celestial mechanics – methods: numerical

1. Introduction

Kepler's equation relates the mean anomaly M and the eccentric anomaly E in orbits with eccentricity e . For elliptic orbits it is given by

$$E - e \sin E = M(E). \quad (1)$$

The function is illustrated for eccentricities 0, 0.1, 0.5, 0.9, and 1 in Fig. 1. It is straight forward to compute $M(E)$. But in practice usually M is given and the inverse function $E(M)$ must be solved.

The innumerable publications about the solution of Kepler's equation (Colwell 1993) highlights its importance in many fields of astrophysics (e.g. exoplanet search, planet formation, star cluster evolution), astrodynamics, and trajectory optimisation. N-body hybrid algorithms also make use of this analytic solution of the two-body problem (Wisdom & Holman 1991). Nowadays, computers can solve Eq. (1) quickly. But the speed increase is counterbalanced by large data sets, simulations, and extensive data analysis (e.g. with Markov chain Monte Carlo). This explains ongoing efforts to accelerate the computation with software and hardware, e.g. by parallelising and usage of GPUs (Graphic Processing Units) (Ford 2009).

Newton-Raphson iteration is a common method to solve Eq. (1) and employs the derivative E' . In each step n the solution is refined by

$$E_{n+1} = E_n + E'(M_n)(M - M_n) = E_n - \frac{E_n - e \sin E_n - M}{1 - e \cos E_n}. \quad (2)$$

A simple starting guess might be $E_0 = M + 0.85e$ (Danby 1987). Each iteration comes at the cost of evaluating one cosine and one sine function. Hence one tries to minimise the number of iterations. This can be done with a better start guess. E.g. Markley (1995) provides a starting guess better than 10^{-4} by inversion of a cubic polynomial which however requires also transcendental functions (4 roots). Boyd (2007) further polynomialised Kepler's equation through Chebyshev polynomial expansion of the sine

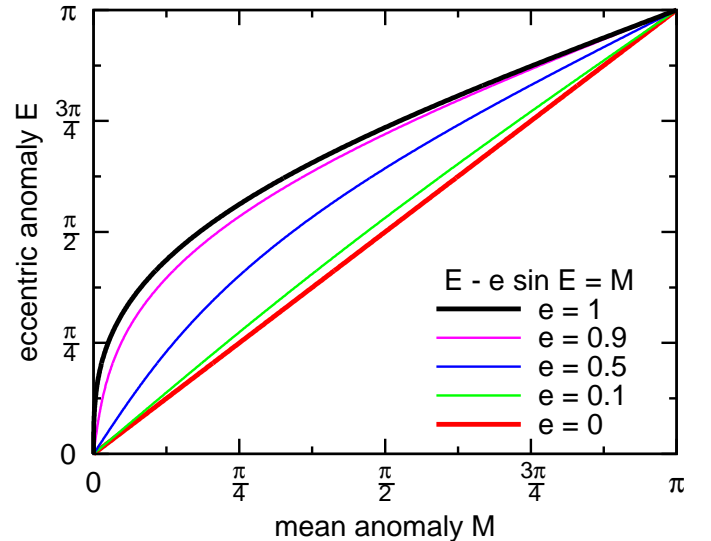


Fig. 1. Kepler's equation for five different eccentricities.

term and yielded with root finding methods a maximum error of 10^{-10} after inversion of a polynomial of degree fifteen. Another possibility to reduce the iteration is to use higher order corrections. For instance Padé approximation of order [1/1] leads to Halley's method.

Precomputed tables can be an alternative way for fast computation of E . Fukushima (1997) used a table equally spaced in E to accelerate a discretised Newton method, while Feinstein & McLaughlin (2006) proposed an equal spacing in M , i.e. a direct lookup table which must be e -dependent and therefore two-dimensional. Both tables can become very large depending on the desired accuracy.

So often the solution of the transcendental Eq. (1) comes back to other transcendental equations which themselves need to

be solved in each iteration. This poses the questions how those often built-in functions are solved and whether there is a way to apply a similar, more direct algorithm to Kepler's equation.

The implementation details of those built-in functions are hardware and software dependent. But sine and cosine are often computed with Taylor expansion. After range reduction and folding into an interval around zero, Taylor expansion is here quite efficient yielding 10^{-16} with 17th degree at $\frac{\pi}{4}$. Kepler's equation can also be Taylor expanded (Stumpff 1968) but that is less efficient, in particular for $e=1$ and around $M = 0$ where the derivative becomes infinite. Similarly, root or arcsine functions are other examples where the convergence of the Taylor expansion is slow. For root-like functions, one again applies Newton-Raphson or bisection methods. The arcsine can be computed as $\arcsin(x) = \arctan\left(\frac{x}{\sqrt{1-x^2}}\right)$ where Taylor expansion of the arctangent function is efficient and one root evaluation is needed.

An interesting alternative method to compute trigonometric functions is the CORDIC (Coordinate Rotation Digital Computer) algorithm which was developed by Volder (1959) for real-time computation of sine and cosine functions and which for instance found application in pocket calculators. CORDIC can compute those trigonometric and other elementary functions in a simple and efficient way.

In this work we will study whether and how the CORDIC algorithm can be applied to Kepler's equation.

2. A scale-free CORDIC algorithm for Kepler's equation

Analogous to CORDIC, we compose our angle of interest, E , by a number of positive or negative rotations $\sigma_i = \pm 1$ with angle α_i

$$E_n = \sum_{i=1}^n \sigma_i \alpha_i. \quad (3)$$

The next iteration n is then

$$E_{n+1} = E_n + \sigma_{n+1} \alpha_{n+1}. \quad (4)$$

The rotation angle α_n is halved in each iteration

$$\alpha_{n+1} = \frac{\alpha_n}{2} = \frac{\alpha_1}{2^n} \quad (5)$$

so that we successively approach E . The direction of the next rotation σ_{n+1} is selected depending on the mean anomaly M_n calculated from E_n via Eq. (1). If $M_n = E_n - e \sin E_n$ overshoots the target value M , then E_{n+1} will be decreased, otherwise increased

$$\sigma_{n+1} = \begin{cases} -1 & E_n - e \sin E_n > M \\ +1 & \text{else.} \end{cases} \quad (6)$$

Equations (4–6) provide the iteration scheme which so far is a binary search or bisection method (with respect to E) to find the inverse of $M(E)$. Choosing as start value $E_0 = 0$ and start rotation $\alpha_1 = \frac{\pi}{2}$, we can cover the range $E \in [-\pi, \pi]$ and precompute the values of rotation angles with Eq. (5)

$$\alpha_n = \frac{\pi}{2^n}. \quad (7)$$

The main difference to the sine CORDIC algorithm is the modified decision for the rotation direction in Eq. (6). There is

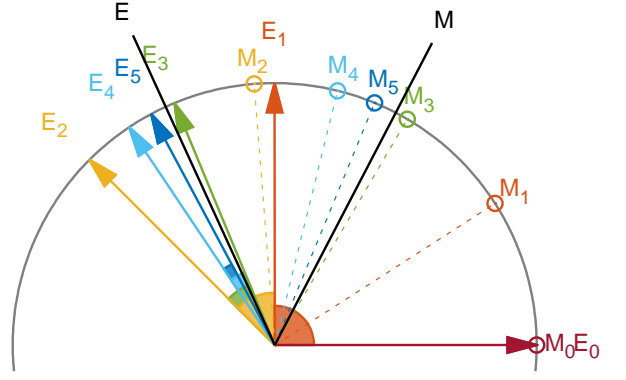


Fig. 2. Example of five CORDIC rotations given $M = 2 - \sin 2 \approx 62.49^\circ$ and $e = 1$. Starting with $M_0 = 0$ and $E_0 = 0$, M_n and E_n approach M and $E = 2 \approx 114.59^\circ$. The arcs indicate the current rotation angle α_n and direction at each step.

the additional term $e \sin E$. For the special case $e = 0$, the eccentric and mean anomalies unify and the iteration converges to $E_n \rightarrow E = M$.

One major key point of CORDIC is that, besides the angle E_n , it propagates simultaneously the Cartesian representation, which are cosine and sine terms of E_n . The next iterations are obtained through trigonometric addition theorems

$$\cos E_{n+1} = \cos(E_n + \sigma_{n+1} \alpha_{n+1}) \quad (8)$$

$$= \cos E_n \cos \alpha_{n+1} - \sigma_{n+1} \sin E_n \sin \alpha_{n+1} \quad (9)$$

$$\sin E_{n+1} = \sin(E_n + \sigma_{n+1} \alpha_{n+1}) \quad (10)$$

$$= \sigma_{n+1} \cos E_n \sin \alpha_{n+1} + \sin E_n \cos \alpha_{n+1}, \quad (11)$$

which is a multiplication with a rotation matrix

$$\begin{pmatrix} c_{n+1} \\ s_{n+1} \end{pmatrix} = \begin{bmatrix} \cos \alpha_{n+1} & -\sigma_{n+1} \sin \alpha_{n+1} \\ \sigma_{n+1} \sin \alpha_{n+1} & \cos \alpha_{n+1} \end{bmatrix} \begin{pmatrix} c_n \\ s_n \end{pmatrix}. \quad (12)$$

Here we introduced the abbreviations $c_n = \cos E_n$ and $s_n = \sin E_n$.

Since the iteration starts with $E_0 = 0$, we have simply $c_0 = \cos E_0 = 1$ and $s_0 = \sin E_0 = 0$. The $\cos \alpha_n$ and $\sin \alpha_n$ terms can also be precomputed using α_n from Eq. (7) and stored in a table listing the triples $(\alpha_n, \cos \alpha_n, \sin \alpha_n)$. Now we have eliminated all function calls for sine and cosine of E and α in the iteration. This is also true and important for the $\sin E_n$ term in Eq. (6) which is simply gathered during the iteration process as s_n via Eq. (12). Figures 2 and 3 illustrate exemplarily the convergence for input $M = 2 - \sin 2 \approx 1.0907$ and $e = 1$ towards $E = 2$.

In Appendix A we provide a little python code which implements the algorithm described in this section. A slightly more elegant formulation is possible with complex numbers $z_n = \exp(iE_n) = \cos E_n + i \sin E_n$ and $a_n = \exp(i\alpha_n) = \cos \alpha_n + i \sin \alpha_n$. Then Eq. (12) becomes $z_{n+1} = a_{n+1} z_n$ or $z_{n+1} = a_{n+1}^* z_n$ depending on σ_n and in Eq. (6) the substitution $\sin E_n = \Im(z_n)$ has to be done.

A more detailed comparison with CORDIC is given Appendix B. Before we analyse performance in Sect. 5.3, we outline some optimisation possibilities in the next section.

3. Variants and refinements

3.1. Minimal rotation base

The algorithms in Sect. 2 and B use always positive or negative rotation directions. While after n rotations the maximum error

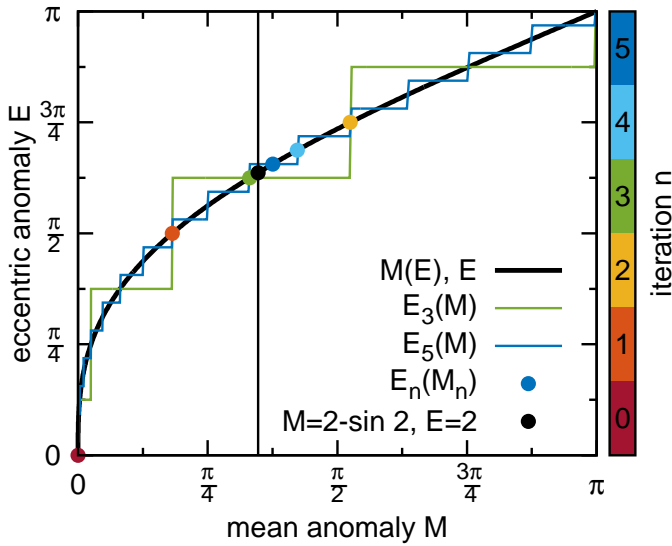


Fig. 3. CORDIC-like approximation of Kepler's equation ($e = 1$). The curves E_3 and E_5 illustrate the convergence towards Kepler's equation after 3 and 5 iterations. The coloured points M_n, E_n are passed during the iterations to find $E(M = 2 - \sin 2)$ (same color-coding as in Fig. 2).

should be smaller than α_n , still previous iterations can be closer to the convergence limit. In Fig. 2, for instance, E_3 is closer to E than E_4 and E_5 . Consecutive rotations will compensate this. A very extreme case is $M = 0$, where $E_0 = 0$ is already the exact value, but the first rotation brings it to $E_1 = 90^\circ$ followed by only negative rotation towards zero.

CORDIC requires positive and negative rotations to have always the same scale K_n after n iterations (Appendix B). But since we could not pull out K_n from the iteration, we can depart from this concept and allow for only zero and positive rotations which could be called unidirectional (Jain et al. 2013) or one-sided (Maharatna et al. 2004). The decision to rotate or not to rotate becomes

$$\sigma_{n+1} = \begin{cases} 1 & (E_n + \alpha_{n+1}) - e \sin(E_n + \alpha_{n+1}) < M \\ 0 & \text{else.} \end{cases} \quad (13)$$

Thereby we will compose E_n in Eq. (3) by minimal rotations and can expect also a better propagation of precision. Moreover, while the term $\sin(E_n + \alpha_{n+1}) = s_n c_a + c_n s_a$ still needs to be computed in each iteration to derive for σ_{n+1} , the term c_{n+1} is updated only when $\sigma_{n+1} = 1$ which will be on average in about 50% of the cases.

Note also that with the minimal rotation base the curve in Eq. (1) is approached from below.

3.2. CORDIC-like Newton method

The convergence of the CORDIC-like algorithms in Sect. 2 and 3.1 is linear, while Newton's method is quadratic. Of course, our algorithm can serve start values (and their cosine and sine terms) for other root finders at any stage. The quadratic convergence should bring the accuracy from, e.g., 10^{-8} down to 10^{-16} at the cost of mainly one division. We think this should be preferred over the other possible optimisations mentioned in Sect. B.

Still, we do not want to lose the ability to provide the cosine and sine terms after one (or more) Newton iterations. We can propagate them simultaneously in a similar manner as in Eqs. (4) and (12) but now using small angle approximations. Newton's

method (Eq. (2)) proposes directly a rotation angle

$$\alpha_{n+1} = E_{n+1} - E_n = \frac{M - E_n + e s_n}{1 - e c_n}. \quad (14)$$

(So there is no need to check for a rotation direction σ_n .) For small angles, there are the approximations $\sin \alpha \approx \alpha$ and $\cos \alpha \approx 1$. If one works with double precision (2^{-53}), the error $\epsilon(\alpha) = |1 - \cos \alpha| < \frac{\alpha^2}{2}$ is negligible, i.e. smaller than $2^{-54} \approx 5.5 \cdot 10^{-17}$, when $|\alpha| < 7.5 \cdot 10^{-9}$ (given for a_{29}). Then we can write

$$c_{n+1} = c_n + \alpha_{n+1} s_n \quad (15)$$

$$s_{n+1} = s_n + \alpha_{n+1} c_n. \quad (16)$$

3.3. Halley's method

Halley's method has a cubic convergence. Ignoring third order terms, one can apply the approximations $\sin \alpha \approx \alpha$ and $\cos \alpha \approx 1 - \frac{\alpha^2}{2}$. The error $\epsilon(\alpha) = |\alpha - \sin \alpha| < \frac{|\alpha^3|}{6}$ is negligible in double precision, when $\alpha < \sqrt[3]{6 \cdot 2^{-54}} = 6.93 \cdot 10^{-6}$ given for $\alpha_{19} \approx 5.99 \cdot 10^{-6}$. Similar to Sect. 3.2, the iteration scheme with corotation for Halley's method is

$$\alpha_{n+1} = \frac{(1 - e c_n)(M - M_n)}{(1 - e c_n)^2 + \frac{1}{2} e s_n (M - M_n)} \quad (17)$$

$$s_{n+1} = \left(1 - \frac{\alpha_{n+1}^2}{2}\right) s_n + \alpha_{n+1} c_n \quad (18)$$

$$c_{n+1} = \left(1 - \frac{\alpha_{n+1}^2}{2}\right) c_n + \alpha_{n+1} s_n. \quad (19)$$

4. Hyperbolic mode

For eccentricities $e \geq 1$, Kepler's equation is

$$M = e \sinh H - H. \quad (20)$$

This case can be treated similar to the elliptic case, when the trigonometric terms are replaced by hyperbolic analogues. Equations (6), (7), and (12) become

$$\sigma_{n+1} = \begin{cases} -1 & e \sinh H_n - H_n > M \\ +1 & \text{else} \end{cases} \quad (21)$$

$$\alpha_n = \frac{4 \ln 2}{2^n} \quad (22)$$

$$\begin{pmatrix} c_{n+1} \\ s_{n+1} \end{pmatrix} = \begin{bmatrix} \cosh \alpha_{n+1} & \sigma_{n+1} \sinh \alpha_{n+1} \\ \sigma_{n+1} \sinh \alpha_{n+1} & \cosh \alpha_{n+1} \end{bmatrix} \begin{pmatrix} c_n \\ s_n \end{pmatrix}. \quad (23)$$

where a sign change in Eq. (23) leads to hyperbolic rotations. This equation set covers a range of $H \in [-4 \ln 2, 4 \ln 2]$. However, H extends to infinity. In the elliptic case, this is handled by an argument reduction which makes use of the periodicity. In hyperbolic case, the corresponding nice base points H_0 are

$$H_0 = m \ln 2 \quad (24)$$

$$c_0 = \cosh H_0 = \frac{1}{2} [\exp H_0 + \exp(-H_0)] = 2^{m-1} + 2^{-m-1} \quad (25)$$

$$s_0 = \sinh H_0 = \frac{1}{2} [\exp H_0 - \exp(-H_0)] = 2^{m-1} - 2^{-m-1}. \quad (26)$$

For $m = 0$, this becomes $H_0 = 0$, $c_0 = 1$, and $s_0 = 0$, i.e. similar as in the elliptic case. For $m \neq 0$, the start triple is still simple to compute using only additions and bitshifts.

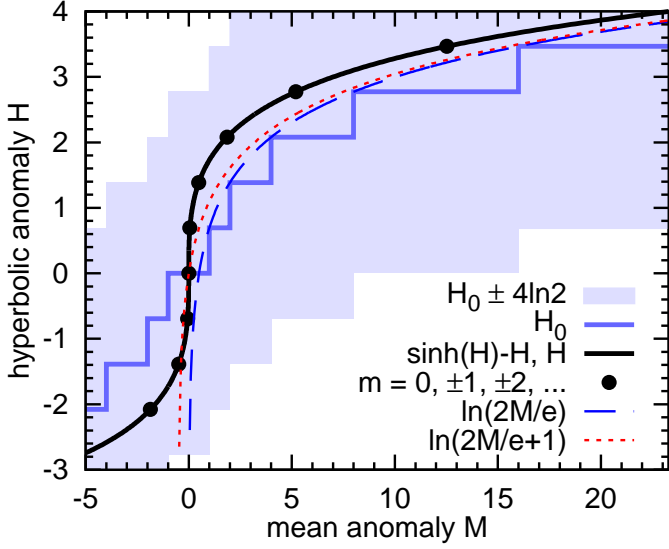


Fig. 4. Range extension for hyperbolic Kepler's equation (black curve) in case $e = 1$. The start value H_0 (blue thick line) and the convergence domain of $\pm 4 \ln 2$ (shaded area) covers Kepler's equation. Nice base points (black dots) and two approximations (dotted and dashed curves) are also indicated.

The main challenge is to obtain the integer m from mean anomaly M . In elliptic case, this needs a division with 2π ; in hyperbolic case, it becomes a logarithmic operation. It is shown in Fig. 4 and Appendix D that

$$m = \text{sign } M \cdot \max \left[0, \text{floor} \left(1 + \log_2 \left| \frac{M}{e} \right| \right) \right] \quad (27)$$

provides start values with the required coarse accuracy of better than $4 \ln 2$. In floating point representation (IEEE 754), the second argument in the maximum function of Eq. (27) extracts simply the exponent of M/e . In fixed point representation, it is the most significant non-zero bit (Walther 1971). This means a logarithm call is not necessary (c.f. Appendix A.2).

The hyperbolic iterations do not return $\cos H$ and $\sin H$, but $\cosh H$ and $\sinh H$ which are the quantities needed to compute distance, velocity, and Cartesian position.

5. Accuracy and performance study

5.1. Accuracy of the minimal rotation base algorithm

The CORDIC-like algorithms have a linear convergence rate. The maximum error for E_n in iteration n is given by α_n . For instance, we expect from Eq. (7) $\alpha_{22} < 10^{-6}$, $\alpha_{29} < 10^{-8}$ (single precision), $\alpha_{42} < 10^{-12}$ and $\alpha_{55} < 10^{-16}$ (double precision). To verify if double precision can be achieved in practice, we forward calculated with Eq. (1) 1000 $(M(E), E)$ pairs uniformly sampled in E over $[0, \pi]$. Here E might be seen as the true value. Then we injected M into our algorithms to solve the inverse problem $E(M)$.

The differences between recomputed and true eccentric anomaly, $\delta_{55} = |E_{55} - E|$, are shown in Fig. 5 for the cases $e = 0.5, 0.9$, and 1. For $M \gtrsim 0.25$ and $e \leq 1$, the deviations are smaller than 10^{-15} and close to machine precision ϵ as indicated by the grey lines. Towards $M = 0$ and $e > 0.9$, the scatter increases. Figure 6 enlarges extremely this corner by plotting the deviations against the logarithm of E for $e = 0.5, 0.9999999999$, and 1.

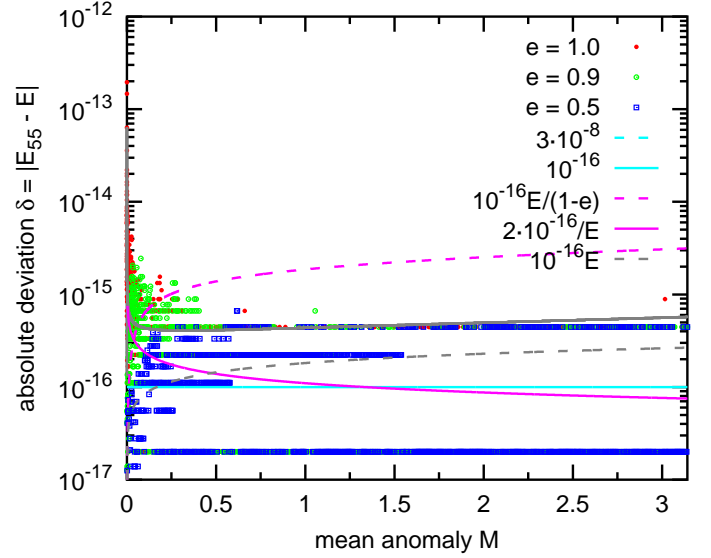


Fig. 5. Accuracy. For visibility, zero deviations ($\delta = 0$) within machine precision were lifted to $\delta = 2 \cdot 10^{-17}$.

The deviations δ_{55} become large in this corner, because the inversion of Eq. (1) is ill-posed. For $e = 1$, third order expansion of Eq. (1) is $M = E - (E - \frac{1}{6}E^3) = \frac{1}{6}E^3$. If the quadratic term in $1 - \frac{1}{6}E^2$ is below machine precision ϵ , it cannot be propagated numerically in the subtraction and leads to a maximum deviation of $E < \sqrt{6\epsilon} \approx 10^{-8}$ at $E = 10^{-8}$ ($M = 10^{-24}$).

Figure 7 illustrates the ill-posed problem. For $e = 1$ and very small M , the cubic approximation provides a very accurate reference. For comparison, we overplot our E_{55} solution as well as computer generated pairs $E - \sin(E), E$. Both exhibit a discretisation of 10^{-8} in E . We conclude that Newton's, Halley's, and other methods which directly try to solve Eq. (1) are as well only accurate to 10^{-8} in this corner when operating with double precision! Therefore, the M, E pairs mentioned above were not generated with built-in $\sin()$ -function but using a Taylor expansion of Kepler's equations

$$M = E(1 - e) - e \left(-\frac{E^3}{3!} + \frac{E^5}{5!} - \dots \right). \quad (28)$$

The term in brackets was called rest function of sine by Stumpff (1959).

We find that the deviations follow approximately the form

$$\delta_{55}(E, e) = |E_{55} - E| \approx 10^{-16} + 10^{-16} \frac{E}{1 - e \cos E} + 10^{-16} E \quad (29)$$

as indicated by the curves in Fig. 5 and 6. For very small M and E , the constant term 10^{-16} dominates. Then the middle term, which is related to the derivative of Eq. (1), sets in. Finally, the linear term $10^{-16}E$ takes over which describes the accuracy to which E can be stored. The middle term leads to an ascending and a descending branch which can be approximated by $10^{-16} \frac{E}{1-e}$ and $10^{-16} \frac{2}{E}$ and forms a local maximum. The two lines intersect at $E \approx \sqrt{2(1-e)}$ and $\delta_{55}(e) \approx 10^{-16} \sqrt{\frac{2}{1-e}}$. For highest resolvable eccentricity below one, this provides $\delta(e = 1 - 10^{-16}) \approx \sqrt{2} \cdot 10^{-8}$.

5.2. Accuracy of algorithm variants

We find that the algorithm with positive and negative rotations (E_n^\pm , Sect. 2) provides a bit worse accuracy for all eccentricities

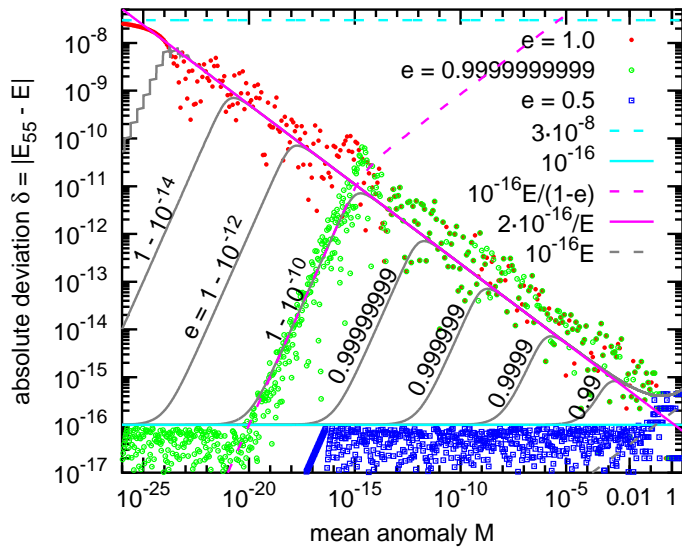


Fig. 6. Similar to Fig. 4, but with logarithmic scaling.

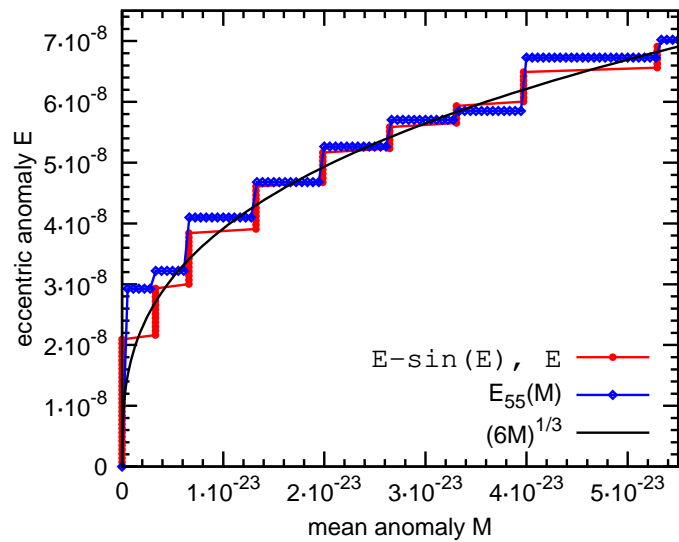


Fig. 7. The ill-posed Kepler equation in the corner $M = 0$ and $e = 1$. Comparison of the computer approximations $M(E) = E - e \sin E$ (red) and our algorithm $E_{55}(M)$ (blue) with a cubic root (black; from well-posed inversion of a third-order Taylor expansion).

(Fig. C.2). For instance for $e = 0.9$, it is limited to 10^{-15} and it ranges up to 10^{-5} for $e = 1$ at $M = 10^{-16}$ ($E = 10^{-5}$).

The combination of one final Newton iteration with E_{29} as suggested in Sect. 3.2 has a similar accuracy as E_{55} (in particular at $e = 1$) and provides therefore an alternative shortcut. The combination of one Halley iteration with E_{19} also performs generally similar, but for high eccentricities it approaches 10^{-6} .

5.3. Performance

Before we discuss some performance results, we have to mention that a comparison of the algorithm speed is not simple. Depending on the hardware, multiplications might be little or much more expensive than additions. Then there is the question about the level of optimisation done in the code, by the compiler, or in built-in routines.

It can be also instructive to count the number of floating point operation. In Appendix A we see 5 multiplications, 4 additions

and one comparison in each iteration. For single precision this needs to be executed 29 times. On the other hand a Newton iteration in Eq. (2) has one division, two multiplications, four additions, and one sine and cosine term. In case the latter two terms are computed via Taylor expansion to 17th order and with a Horner scheme, each will contribute additional 9 multiplications and 9 additions. Furthermore, the cosine and sine routines have to check the need for range reduction each time. Actually, also an additional final sine and cosine operation should be loaded to Newton's methods, since $\sin E$ and $\cos E$ are usually needed in subsequent calculations.

Given same weight to all listed operations, we count about 10 operations per CORDIC iteration vs. about per 43 operation per Newton iteration. Then we estimate that four CORDIC iteration are as expensive as one Newton iteration.

We have implemented both CORDIC-like and Newton's method in a C program. The Newton's method used the start guess $E_0 = M + 0.85e$ and called \cos and \sin function from the standard `math.h` library. The run time was measured with `python timeit` feature for α_{29} (10^{-8}) and for 1000 mean anomalies uniformly sampled from 0 to π . The run-time of the CORDIC-like algorithm is independent of e , while Newton's method is fast for small eccentricities and slower for high eccentricities. We measured that our CORDIC-like method has double, same, and half speed for $e = 1, 0.01, \text{ and } 0$, respectively, or that 14 CORDIC-like iteration are as expensive as one Newton iteration.

5.4. Comparison with Fukushima (1997)

There are some similarities with the work of Fukushima (1997), and a comparison can be enlightening and useful to put our method in context. Fukushima (1997) uses a 128 long table sampled uniformly in E which provides an accuracy of $1/128$. In contrast, we need a table of length $\log_2 128 = 7$ to obtain this accuracy and higher accuracy is not limited by a huge table.

While Fukushima (1997) likely will need fewer iterations due to the use of discretised Newton method, we have no divisions.

Fukushima (1997) developed an iterative scheme with truncated Taylor series of Newton's method to avoid recomputation of sine and cosine angles. Similar, our methods outlined in Sect. 3.2 and 3.3 avoids such recomputations by using truncated Taylor series for sine and cosine for small angles α_n . Our methods appears less complex since it needs only three short equations.

5.5. Universal Kepler's equation

Our algorithms can solve eccentric and hyperbolic Kepler's equation. Both are very similar and could be unified analogous to Walther (1971). Both algorithm includes also the eccentricity $e = 1$ (which are the limits for rectilinear ellipse and hyperbola, i.e. radial cases). The question therefore is, whether our algorithm can be applied to universal Kepler's equation, too.

Following Fukushima (1999) and using the Stumpff function of degree 3, c_3 (Stumpff 1959), the universal Kepler's equation

can be written as

$$L = G + \kappa G^3 c_3(\lambda G^2) \quad (30)$$

$$= G + \kappa \frac{\sqrt{\lambda}G - \sin \sqrt{\lambda}G}{\sqrt{\lambda^3}} \quad (31)$$

$$= G + \kappa \left[\frac{G^3}{3!} - \frac{\lambda G^5}{5!} + \frac{\lambda^2 G^7}{7!} - \dots \right] \quad (32)$$

with universal mean anomaly L , universal eccentric anomaly G , Brunnow's parameter $\lambda = \frac{1-e}{1+e}$, and $\kappa = \frac{e}{1+e}$. In parabolic case ($e = 1$, $\lambda = 0$), it becomes a cubic equation. Using Eq. (31) and the relations $L = \frac{1+\lambda}{2\sqrt{\lambda^3}}M$ and $E = \sqrt{\lambda}G$, one can derive Kepler's equation, Eq. (1) (see Appendix A in Fukushima 1999).

Equation (31) is expressed with a sine term. However, the application of a CORDIC-like algorithm to solve for G seems not possible due to the scaling term $\sqrt{\lambda}$ inside the sine function.

6. Summary

We have shown that the eccentric anomaly E from Kepler's equation can be computed by a CORDIC-like approach and is an interesting alternative to other existing tools. The start vector $E_0 = 0^\circ$ and its Cartesian representation ($\cos E_0 = 1$ and $\sin E_0 = 0$) are rotated using a set of basis angles. The basis angles α_n and its trigonometric function values can be pre-computed and stored in an auxiliary table. Since the table is short and independent of e , it can be also hard-coded.

Our method provides E , $\sin E$, and $\cos E$ without calling any transcendental function at run-time. The precision is adjustable via the number of iterations. For instance, single precision is obtained with $n = 29$ iterations. Using double precision arithmetic, we found the accuracy is limited to $\sim 10^{-15} \sqrt{\frac{2}{1-e}}$ in the extreme corner ($M = 0$, $e = 1$). Regarding accuracy and speed we recommend the one-sided algorithm described in Sect. 3.1.

Our method is very flexible. As a stand-alone method it can provide high accuracy, but it can be also serve start value for other refinement routines and coupled with Newton's and Halley's method. In this context we proposed in Sect. 3.2 and 3.3 to propagate cosine and sine terms simultaneously using small angle approximations in the trigonometric addition theorems and derived the limits when they can be applied without accuracy loss.

Though the number of iterations appears relatively large, the computational load per iteration is small. Indeed, a with simple software implementation we found a competitive performance compared with Newton's method. However, CORDIC algorithms utilise their full potential when implemented in hardware, i.e. directly as digital circuit. So called field programmable gate arrays (FPGA) might be a possibility to install our algorithm closer to machine layout. Indeed, hardware oriented approaches can be very successful. This was shown by the GRAPE (GRAVity PipelinE) project (Hut & Makino 1999), which tackled N-body problems. By implementing Newtonian pair-wise forces efficiently in hardware, it demonstrated a high performance boost and solved new astrodynamical problems (Sugimoto 2003).

Though we could not completely transfer the original CORDIC algorithm to Kepler's equation, it might benefit from ongoing developments and improvement of CORDIC algorithms which is still an active field. In the light of CORDIC, solving Kepler's equations appears almost as simple as computing a sine function.

Acknowledgements. The author thanks the referee Kleomenis Tsiganis for useful comments and M. Kürster and S. Reffert for manuscript reading. This work is supported by the Deutsche Forschungsgemeinschaft under DFG RE 1664/12-1 and Research Unit FOR2544 "Blue Planets around Red Stars", project no. RE 1664/14-1.

References

- Boyd, J. P. 2007, Applied Numerical Mathematics, 57, 12
 Burkardt, T. M. & Danby, J. M. A. 1983, Celestial Mechanics, 31, 317
 Colwell, P. 1993, Solving Kepler's equation over three centuries
 Danby, J. M. A. 1987, Celestial Mechanics, 40, 303
 Feinstein, S. A. & McLaughlin, C. A. 2006, Celestial Mechanics and Dynamical Astronomy, 96, 49
 Ford, E. B. 2009, New A, 14, 406
 Fukushima, T. 1997, Celestial Mechanics and Dynamical Astronomy, 66, 309
 Fukushima, T. 1999, Celestial Mechanics and Dynamical Astronomy, 75, 201
 Hachiaichi, Y. & Lahbib, Y. 2016, ArXiv e-prints [arXiv:1606.02468]
 Hut, P. & Makino, J. 1999, Science, 283, 501
 Jain, A., Khare, K., & Aggarwal, S. 2013, International Journal of Computer Applications, 63, 1, full text available
 Maharatna, K., Troya, A., Banerjee, S., & Grass, E. 2004, IEE Proceedings - Computers and Digital Techniques, 151, 448
 Markley, F. L. 1995, Celestial Mechanics and Dynamical Astronomy, 63, 101
 Stumpff, K. 1959, Himmelsmechanik.
 Stumpff, K. 1968, Rep. NASA Tech. Note, NASA-TN-D-4460, 29 p., 4460
 Sugimoto, D. 2003, in IAU Symposium, Vol. 208, Astrophysical Supercomputing using Particle Simulations, ed. J. Makino & P. Hut, 1
 Volder, J. E. 1959, IRE Transactions on electronic computers, 330
 Walther, J. S. 1971, in Proceedings of the May 18-20, 1971, Spring Joint Computer Conference, AFIPS '71 (Spring) (New York, NY, USA: ACM), 379-385
 Wisdom, J. & Holman, M. 1991, AJ, 102, 1528

Appendix A: A python code for illustration

The following codes implement the two-sided algorithms described in Sect. 2 and 4.

Appendix A.1: Elliptic case

```

1 # initialise cos-sin look-up table
2 from math import pi, cos, sin, floor
3 divtwopi = 1 / (2*pi)
4 acs = [(a, cos(a), sin(a)) for a in \
5         [pi/2**i for i in range(1,60)]]
6
7 def Ecs(M, e, n=29):
8     E = 2 * pi * floor(M*divtwopi+0.5)
9     cosE, sinE = 1., 0.
10    for a, cosa, sina in acs[:n]:
11        if E-e*sinE > M:
12            a, sina = -a, -sina
13            E += a
14            cosE, sinE = cosE*cosa - sinE*sina, \
15                        cosE*sina + sinE*cosa
16    return E, cosE, sinE

```

As an example, calling the function with `Ecs(2 - sin(2), 1)` should return the triple `(1.99999999538762, -0.4161468323531165, 0.9092974287451092)`.

Note, this pure python code shall illustrate the functionality and low complexity (not performance). An implementation in C (including a wrapper to python) and gnuplot with algorithm variants (e.g. one-sided for improved accuracy and speed) are online available¹.

¹ <https://github.com/mzechmeister/ke>

Appendix A.2: Hyperbolic case

```

1 # initialise cosh-sinh look-up table
2 from math import log, cosh, sinh, frexp, ldexp
3 ln2 = log(2)
4 acsh = [(a, cosh(a), sinh(a)) for a in \
5         [4*ln2/2**i for i in range(1,60)]]
6
7 def Hcs(M, e, n=29):
8     m = max(0, frexp(M/e)[1])
9     if M < 0: m = -m
10    H = m * ln2
11    coshH = ldexp(1, m-1) + ldexp(1, -m-1)
12    sinhH = ldexp(1, m-1) - ldexp(1, -m-1)
13    for a, cosha, sinha in acsh[:n]:
14        if e*sinhH-H > M:
15            a, sinha = -a, -sinha
16            H += a
17            coshH, sinhH = coshH*cosha + sinhH*sinha, \
18                          coshH*sinha + sinhH*cosha
19    return H, coshH, sinhH

```

Calling `Hcs(sinh(2)-2, 1)` returns the triple (1.9999999991222275, 3.7621956879000753, 3.626860404544669).

The function `frexp` returns the mantissa and the exponent of a floating point number. Vice versa, the function `ldexp` needs a mantissa and an exponent to create a floating point number.

Appendix B: Comparison with original CORDIC algorithm for the sine

The CORDIC algorithm for the sine function is in practice further optimised to work solely with additive operation and bitshift operation and without multiplication or even division. The rotation angles α_n are slightly modified for this purpose such that now for $n > 1$

$$\tan \alpha_n = \frac{1}{2^{n-2}}. \quad (\text{B.1})$$

As in the previous Sect. 2, the first iteration starts with $\alpha_1 = 90^\circ$ ($\tan \alpha_1 = \infty$). The second angle is also the same $\alpha_2 = 45^\circ$ ($\tan \alpha_2 = 1$), while all other angles are somewhat larger than in Eq. (7) and the convergence range is $\sum_{n=1}^{\infty} \alpha_n = 1.0549\pi = 189.9^\circ$. Using Eq. (B.1) we can write Eq. (12) as

$$\begin{pmatrix} c_{n+1} \\ s_{n+1} \end{pmatrix} = \cos \alpha_{n+1} \begin{bmatrix} 1 & -\sigma_{n+1} \frac{1}{2^{n-1}} \\ \sigma_{n+1} \frac{1}{2^{n-1}} & 1 \end{bmatrix} \begin{pmatrix} c_n \\ s_n \end{pmatrix}. \quad (\text{B.2})$$

The next trick in CORDIC is to take out the factor $\cos \alpha_n$ from this equation and to accumulate it separately. This saves two multiplications, but changes the magnitude of the vector by $\cos \alpha_n$ in each iteration and after n iteration by

$$K_n = \prod_{i=2}^n \cos \alpha_i = \prod_{i=2}^n \frac{1}{\sqrt{1 + \tan^2 \alpha_i}} = \prod_{i=0}^{n-2} \frac{1}{\sqrt{1 + 4^{-i}}}. \quad (\text{B.3})$$

This scale correction factor K_n can be applied once after the last iteration. The iteration scheme for the scale dependent vector X_n, Y_n (where $c_n = K_n X_n$ and $s_n = K_n Y_n$) becomes

$$X_{n+1} = X_n - Y_n \frac{\sigma_{n+1}}{2^{n-1}} \quad (\text{B.4})$$

$$Y_{n+1} = Y_n + X_n \frac{\sigma_{n+1}}{2^{n-1}} \quad (\text{B.5})$$

This could be applied for the solution of Eq. (1), too. However, the check for rotation direction in Eq. (6) requires then a scale correction ($E_n - eK_n X_n > M$). So one multiplication remains, while one multiplication can still be saved. The additional multiplication with e could be saved by including it into the start vector (i.e. $z_0 = e \exp(iE_0) = e = X_0$ for $E_0 = 0$).

The final trick in CORDIC is to map float values to integer values which has the great advantage that the division by a power of 2 can be replaced by bit shifts. But since we could not eliminate all multiplications, the full concept of CORDIC is unfortunately not directly applicable to solve Kepler's equation. Therefore, we call our method CORDIC-like.

However, it should be noted that also scale free CORDIC algorithms have been developed (Hachaichi & Lahbib 2016) at the expense of some additional bitshift operations. Furthermore, the scale correction K_n , which converges to $K_\infty \approx 0.607253 \approx 1/1.64676$, does not change in double precision for $n = 26$. This means from iteration $n = 26$ onwards, the concept of CORDIC is applicable, when setting the magnitude of the start vector to $K_{26}e$. Similar, for $n = 29$, the cosine term becomes one in double precision ($\cos \alpha_n = 1$), which also indicates a quasi-constant scale factor and means that we can save this multiplication. In Sect. 3.2 and 3.3 we exploit this fact in another way.

Appendix C: Accuracy plots

Appendix D: Start guess in hyperbolic case

It can be shown that Eq. (27) always provides a lower bound for H in case of $M \geq 0$. Starting with Kepler's equation Eq. (20) and using the identity $\sinh x = \frac{1}{2}[\exp x - \exp(-x)]$ and the inequality $\exp(-x) \geq 1 - 2x$ (for $x \geq 0$), we obtain

$$\begin{aligned} M &= e \sinh H - H = \frac{e}{2} \left[\exp H - \exp(-H) - 2 \frac{H}{e} \right] \\ &\leq \frac{e}{2} \left[\exp H - 1 + 2H \left(1 - \frac{1}{e} \right) \right] \\ &\leq \frac{e}{2} [\exp H - 1]. \end{aligned}$$

For large values H , the approximation becomes more accurate. Further reforming and introduction of the binary logarithm yields

$$H \geq \ln \left(\frac{2M}{e} + 1 \right) = \ln 2 \cdot \log_2 \left(\frac{2M}{e} + 1 \right). \quad (\text{D.1})$$

The right side of Eq. (D.1) is plotted in Fig. 4 as a red dotted line. It belongs to the family of start guesses given in Burkardt & Danby (1983) ($H_0 = \ln(\frac{2M}{e} + k)$). For $\frac{M}{e} = \frac{1}{2}$, $e = 1$, and $H_0 = 0$, the deviation is $H - H_0 \approx 1.396 = 2.014 \ln 2$. Since, unfortunately, the prefactor is slightly larger than two, the convergence range is expanded to $4 \ln 2$ by setting $\alpha_1 = 2 \ln 2$ in Eq. (22).

For this large convergence range, we can further simply the start guess by omitting the additive one in Eq. (D.1)

$$H > \ln \frac{2M}{e} = \ln 2 \cdot \log_2 \frac{2M}{e} = \ln 2 \cdot \left(1 + \log_2 \frac{M}{e} \right) \quad (\text{D.2})$$

$$> \ln 2 \cdot \text{floor} \left(1 + \log_2 \frac{M}{e} \right) \quad (\text{D.3})$$

which finally leads to the start value for m in Eq. (27). The right function in Eq. (D.2) is plotted in Fig. 4 as a blue dashed line.

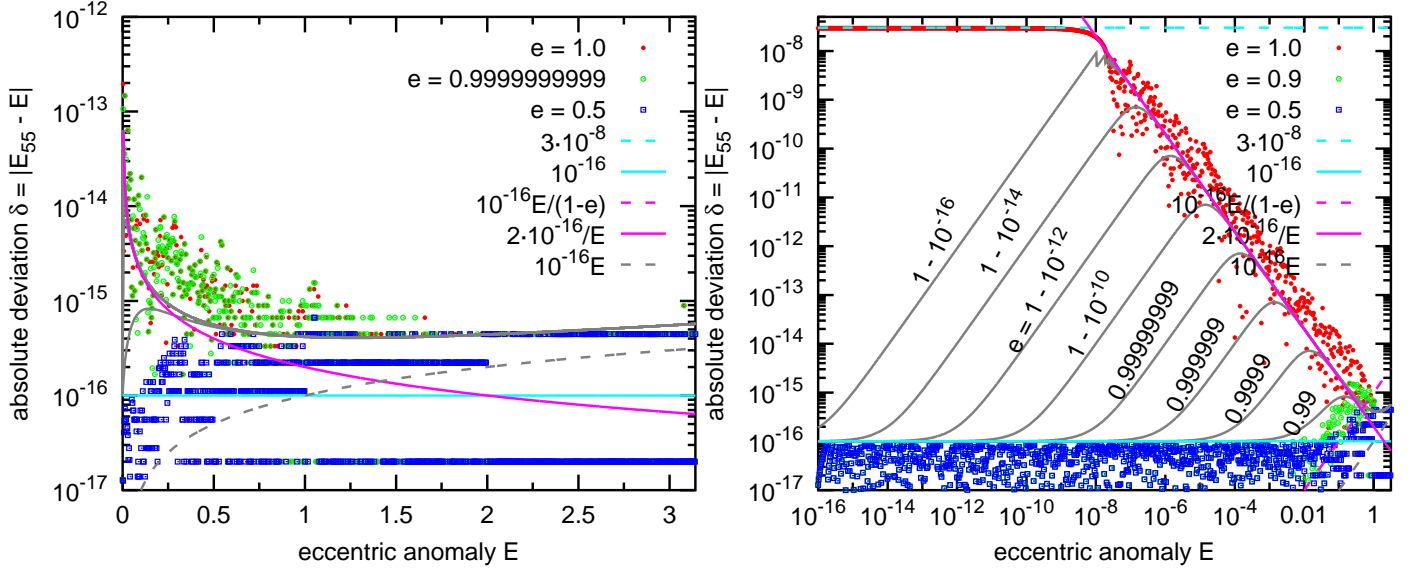


Fig. C.1. Similar to Figs. 5 and 6, but as function of E .

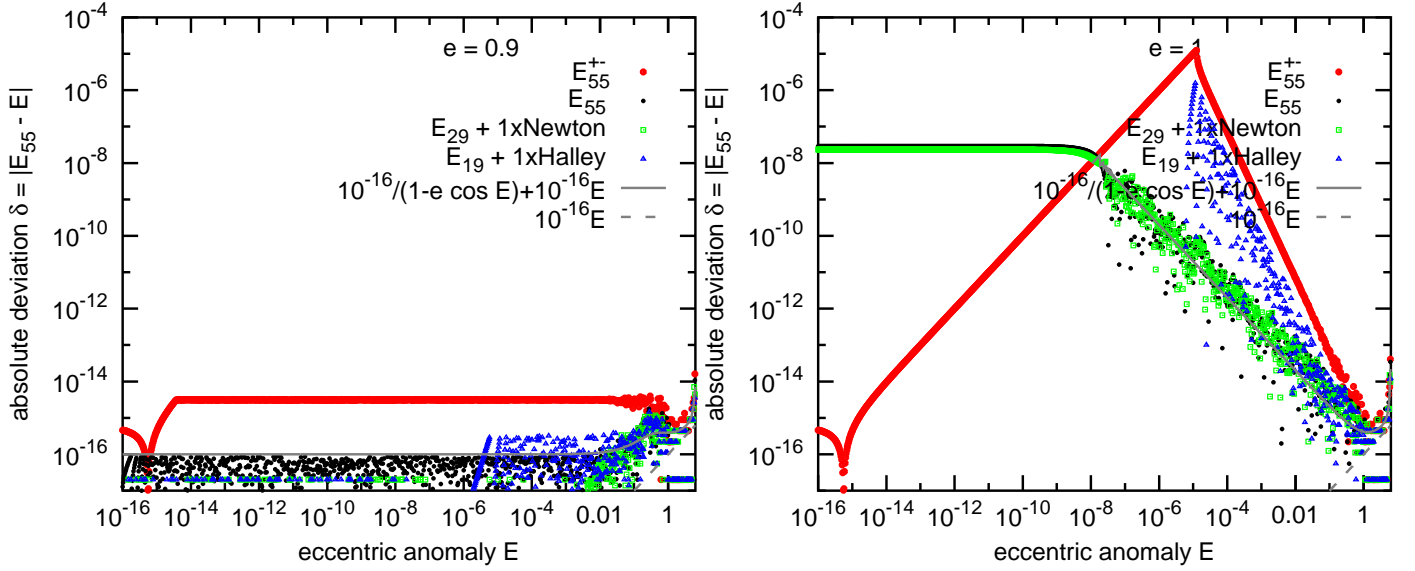


Fig. C.2. Accuracy comparison of algorithm variants.

At $\frac{M}{e} = 1$ and $e = 1$, the hyperbolic anomaly is $H \approx 1.729 = 2.495 \ln 2$ and thus inside our convergence domain.

The simple start guess developed here is valid for all $e \geq 1$ and a lower bound for $M \geq 0$, i.e. suitable for one-sided algorithms.